Clim. Past Discuss., doi:10.5194/cp-2016-48, 2016
Manuscript under review for journal Clim. Past
Published: 26 April 2016

Climate of the Past Discussions
Open Access
EGU

Greenland warming during the last interglacial: the relative importance of insolation and oceanic changes

Rasmus A. Pedersen[1,2], Peter L. Langen[2], and Bo M. Vinther[1]

[1]Centre for Ice and Climate, Niels Bohr Institute, University of Copenhagen, Copenhagen, Denmark
[2]Climate and Arctic Research, Danish Meteorological Institute, Copenhagen, Denmark

Correspondence to: Rasmus A. Pedersen (anker@nbi.ku.dk)

Abstract. Insolation changes during the Eemian (the last interglacial period, 129–116,000 years before present) resulted in warmer than present conditions in the Arctic region. The NEEM ice core record suggests warming of 8±4 K in northwestern Greenland based on water stable isotopes. Here we use general circulation model experiments to investigate the causes of the Eemian warming in Greenland. Simulations of the atmospheric response to combinations of Eemian insolation and pre-industrial oceanic conditions and vice versa, are used to disentangle the impacts of the insolation change and the related changes in sea surface temperatures and sea ice conditions. The changed oceanic conditions cause warming throughout the year, prolonging the impact of the summertime insolation increase. Consequently, the oceanic conditions cause annual mean warming of 2 K at the NEEM site, whereas the insolation alone causes an insignificant change. Taking the precipitation changes into account, however, the insolation and oceanic changes cause more comparable increases in the precipitation-weighted temperature, implying that both contributions are important for the ice core record at the NEEM site. The simulated Eemian precipitation-weighted warming of 2.4 K at the NEEM site is low compared to the ice core reconstruction, partially due to missing feedbacks related to ice sheet changes. Surface mass balance calculations with an energy balance model indicate potential mass loss in the north and southwestern parts of the ice sheet. The oceanic conditions favor increased accumulation in the southeast, while the insolation appears to be the dominant cause of the expected ice sheet reduction.

1 Introduction

The last interglacial, the Eemian, was characterized by higher than present temperatures in the Arctic region driven by increased summertime insolation at high northern latitudes (CAPE-Last Interglacial Project Members, 2006; Masson-Delmotte et al., 2013). The recent NEEM ice core from northwestern Greenland covers the last interglacial period and indicates substantial warming from 129–114 thousand years before present (ka) peaking at 8±4 K above the mean of the last millennium (NEEM community members, 2013). This temperature estimate is based on stable water isotopes, specifically δ^{18}O, using the temperature–isotope relation from the present interglacial (Vinther et al., 2009). A recent, alternate reconstruction based on isotopic air composition (δ^{15}N) from the same ice core yields a very similar estimate of 7–11 K, with 8 K as the most likely estimate (Landais et al., 2016). General circulation models, however, generally simulate a much more limited warming (Bra-

Clim. Past Discuss., doi:10.5194/cp-2016-48, 2016
Manuscript under review for journal Clim. Past
Published: 26 April 2016

connot et al., 2012; Lunt et al., 2013; Masson-Delmotte et al., 2013; Otto-Bliesner et al., 2013), motivating further investigation of the mechanisms behind the Eemian warming in Greenland.

During the Eemian, the global sea level was increased 6–9 m above present (Dutton and Lambeck, 2012; Dutton et al., 2015; Kopp et al., 2009), indicating a substantial reduction of the continental ice sheets. Several studies have presented ice sheet model reconstructions of the Greenland ice sheet (GrIS), but the reconstructions vary substantially in both magnitude and spatial distribution of the ice sheet changes. Regarding the magnitude, the ensemble of reconstructions suggests a likely range of sea level contribution from GrIS of 1.4–4.3 m (Masson-Delmotte et al., 2013). Spatially, the potential changes as suggested by the various models are retreat in southwest (Helsen et al., 2013), retreat in north- and southwest with a separate South Dome ice cap (Robinson et al., 2011), retreat in southwest and north-northeast (Born and Nisancioglu, 2012; Quiquet et al., 2013; Stone et al., 2013), and complete loss of the South Dome (Cuffey and Marshall, 2000; Lhomme et al., 2005). Only very few constraints exist that can be used to assess these reconstructions. The deep Greenland ice cores that contain Eemian ice are obvious fix-points. These are NEEM (77.45° N, 51.06° W; NEEM community members (2013)), NGRIP (75.10° N, 42.32° W; NGRIP members (2004)), GRIP (72.5° N, 37.3° W; GRIP members (1993)) and GISP2 (72.58° N, 38.48° W; Grootes et al. (1993)). Additionally, basal parts of the Renland (71.3° N, 26.7° W) and Camp Century (77.2° N 61.1° W) ice cores contain ice from the Eemian (Johnsen et al., 2001). The DYE-3 ice core further south (65.2° N 43.8° W, Dansgaard et al. (1982)) has distorted layers making it difficult to assess the deepest part of the core (Johnsen et al., 2001), but the basal part contains ice older than the Eemian (Willerslev et al., 2007). Ocean sediment cores further indicate the presence of ice in southern Greenland during the Eemian (Colville et al., 2011).

Due to the lapse rate (i.e. decreasing temperature with atmospheric height), elevation changes will impact the surface temperature on GrIS. While the ice core air content only suggests limited elevation changes at the NEEM site (45±350 m higher than present ice sheet elevation), the NEEM ice core temperature reconstruction has been corrected using the surface elevation change estimate from the ice core air content (NEEM community members, 2013). Besides the direct impact of the elevation change, changes in the GrIS topography could also impact the large scale circulation (Hakuba et al., 2012; Lunt et al., 2004; Petersen et al., 2004), as well as the local conditions on Greenland (Merz et al., 2014a) and the ice core record through changed precipitation patterns (Merz et al., 2014b).

The conversion from δ^{18}O to temperature may be a contributing factor to mismatches between model simulations and δ^{18}O temperature reconstructions: The δ^{18}O–temperature relationship is sensitive to precipitation intermittency, evaporation conditions, and atmospheric transport, and thus varies spatially and historically (Jouzel et al., 1997; Masson-Delmotte et al., 2011). Hence, sea surface warming and reduced sea ice extent might thus affect the δ^{18}O record, as illustrated by isotope-enabled climate model simulations (Sime et al., 2013). The NEEM δ^{18}O temperature estimate is based on the average Holocene δ^{18}O–temperature relationship from other central Greenland ice cores (Vinther et al., 2009), but the actual relationship might be different due to the shifted location or the climatic changes during the Eemian.

One important factor to consider when interpreting ice core records is the precipitation seasonality. The ice core record reflects the snow deposition on the surface, and thus only records climatic information during snowfall events (Steig et al., 1994). The precipitation seasonality thus creates a bias towards seasons with more snow deposition, and changes in the seasonality

Clim. Past Discuss., doi:10.5194/cp-2016-48, 2016
Manuscript under review for journal Clim. Past
Published: 26 April 2016

Climate of the Past Discussions
Open Access
EGU

may induce changes in the ice core record even with an unchanged temperature (Persson et al., 2011). As an example, model simulations indicate that the present day climate in northwestern Greenland is biased towards summer due to precipitation seasonality (Steen-Larsen et al., 2011). Thus, when comparing model simulations to ice core records it is useful to consider the precipitation-weighted temperature to obtain a fair comparison. The precipitation-weighted temperature (T_{pw}) can be calculated as:

$$T_{pw} = \frac{\sum_{j=1}^{N} T_j p_j}{\sum_{j=1}^{N} p_j} \tag{1}$$

where N denotes the total number of time samples, and T_j and p_j is the temperature and precipitation during the jth time sample. In our study, the weighting is based on monthly means of near surface air temperature and total precipitation.

Using a series of general circulation model (GCM) experiments, we assess the GrIS warming during the Eemian. Specifically, we aim to compare the direct impact of the insolation change and the indirect effect of retreating sea ice and increasing sea surface temperatures (SSTs). We investigate how the simulated changes could affect the GrIS surface mass balance and the ice core record, and whether the insolation or the oceanic changes dominate the total response.

The experiments and the employed models are described in Sect. 2. Results are presented and discussed in Sect. 3, followed by conclusions in Sect. 4.

2 Methods

2.1 Model configuration

The model used for this study is the EC-Earth global climate model in the most recent version 3.1 (Hazeleger et al., 2010, 2012). We employ the atmosphere-only configuration based on the IFS atmospheric model (cycle 36r4, European Centre for Medium-Range Weather Forecasts (2010)) in a T159 spectral resolution with an associated Gaussian grid of roughly 1.125° × 1.125° horizontal resolution and 62 layers in the vertical. In order to allow paleoclimate simulation, the model has been expanded with an option to modify the insolation according to any given orbital configuration. The insolation is internally calculated following Berger (1978) using the same code modification as Muschitiello et al. (2015).

The prescribed sea surface boundary conditions (sea surface temperature and sea ice concentration) are obtained from two simulations with the fully-coupled EC-Earth system: an Eemian experiment forced with 125 ka conditions (i.e. insolation and greenhouse gas concentrations; GHGs) and a pre-industrial control experiment. The coupled experiments are described and presented in Pedersen et al. (2016b).

Due to the diverse ice sheet reconstructions, we have kept the ice sheets fixed at present day extents in all of our simulations. Vegetation is similarly kept at present day values, and consequently our experiments do not include any additional feedbacks from vegetation or ice sheet geometry (as discussed in Pedersen et al. (2016b)).

Clim. Past Discuss., doi:10.5194/cp-2016-48, 2016
Manuscript under review for journal Clim. Past
Published: 26 April 2016

2.2 Surface mass balance calculations

To investigate the impacts of the simulated climate changes on the GrIS surface mass balance, we performed off-line calculations with the subsurface scheme of the HIRHAM5 regional climate model (updated from Langen et al. (2015)). The subsurface model was here run on the Gaussian grid associated with the EC-Earth experiments and forced at 6 hour intervals with incoming shortwave and downward longwave radiation, latent and sensible heat fluxes, along with rain, snow and evaporation/sublimation taken directly from the EC-Earth output. The subsurface model was updated slightly compared to that described by Langen et al. (2015); most notably it employs 25 layers with a total depth of 70 m water equivalent and includes temperature- and pressure-dependent densification of snow and firn (following Vionnet et al. (2012)). It accounts for heat diffusion, vertical water transport and refreezing. Each layer can hold liquid water corresponding to 2 % of the snow pore space volume and excess water percolates downward to the next layer. When a layer density exceeds the pore close off density (830 kg m^{-3}), water percolating down from above is added to a slush layer and runs off exponentially with an exponential time scale depending on surface slope (Lefebre et al., 2003; Zuo and Oerlemans, 1996). Until it runs off, the slush layer water is available for superimposed ice formation onto the underlying ice layer at a rate that assumes a linear temperature profile in that layer.

2.3 Experimental design

We have designed four experiments to investigate how the last interglacial insolation changes impacted the climatic conditions on Greenland (cf. Table 1). An experiment with Eemian (125 ka) conditions ("iL+oL") is compared to a pre-industrial control climate state ("iP+oP"). The simulations are forced with GHGs and insolation from the respective periods along with prescribed sea surface temperatures (SST) and sea ice concentration (SIC) obtained from fully coupled model experiments with identical GHGs and insolation. Ice sheets and vegetation are kept at pre-industrial conditions in both experiments. Aiming to disentangle the direct impact of the insolation changes and the secondary impact of changed sea surface conditions (SST and SIC), we have designed two hybrid experiments: The first experiment is forced by Eemian insolation and pre-industrial sea surface conditions ("iL+oP") and the second is conversely forced by pre-industrial insolation and Eemian sea surface conditions ("iP+oL").

During the Eemian at 125 ka the Northern Hemisphere summer solstice occurs near perihelion and the obliquity is increased compared to present day. The changed orbit causes an insolation increase over Greenland during summer compensated by a decrease during autumn, i.e. an earlier onset of the polar night (cf. Fig. 1).

The changed insolation leads to sea ice retreat and increasing SSTs across high northern latitudes (see detailed description in Pedersen et al. (2016b)). Figure 2 depicts the sea ice retreat and the SST anomalies from the coupled simulations, indicating the differences between the sea surface boundary conditions. The sea ice reduction is primarily manifested as a northward retreat of the ice edge (as illustrated by the sea ice extent contours in Fig. 2); the sea ice concentration in the central Arctic is largely unchanged (not shown).

Clim. Past Discuss., doi:10.5194/cp-2016-48, 2016
Manuscript under review for journal Clim. Past
Published: 26 April 2016

Climate of the Past Discussions

All simulations have a total length of 60 years of which the 10 first years are disregarded as spin-up. Statistical significance of changes is assessed using a two-sided Student's t test (von Storch and Zwiers, 2001), taking into account the serial autocorrelation of the time series.

3 Results and Discussion

As described by Pedersen et al. (2016b), the anomalies between Eemian and pre-industrial conditions in the atmosphere-only model configuration closely resemble those of the fully coupled experiments. Figure 3 shows that entire Greenland warms in all seasons in the full Eemian experiment, iL+oL. The peak warming is generally found in the coastal regions, but the central, high altitude Summit region warms more than 2 K in both summer (June-July-August; JJA) and winter (December-January-February; DJF). During summer, strong warming patches are collocated with loss of snow cover (not shown). Increased shortwave absorption and a consequent larger sensible heat flux from the surface indicates that surface albedo changes are contributing to these local warming peaks.

The hybrid simulations, iP+oL and iL+oP, exhibit very different annual cycles of warming. Following the insolation changes, iL+oP only shows warming during summer covering the entire Greenland, whereas fall (September-October-November; SON) and winter exhibit cooling; the winter cooling is limited to the southwestern part of Greenland. A small area in northwestern Greenland is warming through winter and spring (March-April-May; MAM). Again, this warming coincides with loss of snow cover, and increased sensible heat release from the surface. Continental snow cover changes can thus extend the summertime warming to the colder seasons with reduced insolation, but the iL+oP experiment indicates that this memory effect only plays a minor role for GrIS as a whole.

The oceanic changes in iP+oL cause warming over entire Greenland, peaking in the colder seasons fall and winter. Warming due to sea ice loss peaks during winter, following increased turbulent heat flux from the ocean surface where the insulating sea ice layer is lost [in agreement with previous studies of sea ice loss (Pedersen et al., 2016a; Vihma, 2014)]. Previous studies show that the GrIS near surface temperature is sensitive to sea ice changes in its vicinity (Pedersen et al., 2016a), and that ice loss in the Nordic Seas could have a larger impact than ice loss in the Labrador Sea due to an atmospheric circulation response (Merz et al., 2016). Additional SST increase from ocean circulation changes and increased summertime shortwave absorption (Pedersen et al., 2016b) expands the regions with positive turbulent heat flux anomalies beyond the areas of sea ice loss (not shown). The total impact of the oceanic changes thus counters the direct impact of the insolation during fall and winter, resulting in the all-year warming observed in iL+oL, which closely resembles the sum of the iP+oL and iL+oP.

Similar to the temperature, the snowfall over GrIS also exhibits varying sensitivity to the insolation and the oceanic changes (cf. Fig. 4). The simulated responses reveal that the ice sheet topography is important for the precipitation changes: Figure 4 reveals several examples of contrasting snowfall changes on the east and western side of the ice divide. In iL+oL, the southern Greenland snowfall is increased throughout the year. The west coast appears drier during summer due to an increasing fraction of the precipitation falling as rain; the total precipitation is increased along the coast (not shown). The entire interior ice sheet receives more snow during summer, while the eastern (western) part have increased snowfall during fall (spring). The hybrid

Clim. Past Discuss., doi:10.5194/cp-2016-48, 2016
Manuscript under review for journal Clim. Past
Published: 26 April 2016

experiments reveal that the snowfall increase primarily is driven by the oceanic changes (cf. iP+oL). iL+oL and iP+oL have high resemblance, especially winter and spring, while the insolation appears to contribute to the snowfall increase over the interior ice sheet during summer. The fall pattern in iL+oL on the other hand indicates non-linear behavior, in that iL+oL does not resemble the sum of the two hybrid experiments: the strong increase on the western GrIS is only seen in iL+oL.

3.1 Precipitation-weighted temperature

The precipitation changes in Fig. 4 suggest that the northwestern GrIS near the NEEM ice core location is affected by changed precipitation seasonality in all three simulations: the insolation in iL+oP causes increased summer snowfall and drier conditions in fall, the oceanic changes in iP+oL cause increased snowfall throughout the year, and the combination in iL+oL leads to increased snowfall during spring and summer. To assess how these changes might affect the ice core record, the precipitation-weighted annual mean temperature has been calculated following Eq. (1); Figure 5 compares the annual mean temperature change and the precipitation-weighted mean.

The precipitation-weighted mean temperature (T_{pw}) in iL+oL is relatively similar to the annual mean (T_{ann}). One exception is the northwestern GrIS, where T_{pw} is higher suggesting a strong bias towards summer in the precipitation seasonality. The widespread, general precipitation increase driven by the changed oceanic conditions in iP+oL only causes minor differences between the annual and the precipitation-weighted means: The precipitation-weighting primarily affects the near-coastal regions. Conversely, iL+oP exhibits a large difference between T_{ann} and T_{pw}. The combination of wetter summer conditions and drier conditions during winter and fall in western Greenland, increases T_{pw} in a large region covering the central, west, and northwest GrIS. By comparing the hybrid simulations to the response in iL+oL, it appears that the insolation changes are responsible for the changed precipitation seasonality that causes the increased T_{pw} in the northwestern GrIS.

Due to the flow of the ice, the deposition site of the Eemian ice from the NEEM ice core is further upstream than the drilling location (approximately 76.4° N, 44.8° W, 205±20 km upstream; NEEM community members (2013)). To ensure fair comparison, we consider the simulated conditions over this point (dNEEM) when comparing model results and ice core records (note, however, that the upstream correction is within two grid cells). Table 2 presents the annual mean and precipitation-weighted temperatures for dNEEM, revealing a varying impact between the three simulations. The iL+oL estimate is largely unchanged by the precipitation-weighting, and is thus still relatively low compared to the ice core temperature reconstructions. As evident from Fig. 5, the precipitation-weighted temperature north-northwest of dNEEM exhibits a higher increase, but the strongest does not exceed 3–4 K.

From the annual mean temperatures, the SST and sea ice changes (iP+oL) appear to completely dominate the temperature change at dNEEM. Taking the precipitation seasonality into account, however, reveals that the direct impact of the insolation has a comparable contribution to the warming signal recorded in the ice core.

The three experiments indicate substantial non-linearity in the responses to the changed insolation and oceanic conditions. While iP+oL indicates that SST and sea ice changes results in a warming of 1.5 K (ΔT_{pw}) at the NEEM location, the difference between iL+oL and iL+oP suggests that the oceanic changes only contribute with 0.8 K (ΔT_{pw}) additional warming.

Clim. Past Discuss., doi:10.5194/cp-2016-48, 2016
Manuscript under review for journal Clim. Past
Published: 26 April 2016

3.2 GrIS surface mass balance

Both the increasing temperature and the general precipitation increase could be important for a potential reduction of the Greenland ice sheet. While the ice sheet is fixed in our experiments, the offline calculations with the subsurface model presents an estimate of the combined effect of the warming and precipitation changes over GrIS. The surface mass balance (SMB) is the sum of accumulation and ablation (i.e. run-off) calculated in each grid cell based on 6-hourly output from the EC-Earth experiments (incoming shortwave and downward longwave radiation, latent and sensible heat fluxes, rain, snow and evaporation/sublimation). As EC-Earth does not have an explicit glacier mask, we have performed the calculations in all grid cells with a minimum snow depth of 10 cm across all the simulations. Consequently, our estimates likely do not capture the full ablation zone, where the snow cover would melt every year. Therefore, we do not consider the integrated SMB, but only the spatial pattern. Figure 6 shows the resulting SMB changes in the three simulations compared to iP+oP.

The SMB change in iL+oL reveals a general decrease along the coast extending further inland in the north combined with increased values along the southeast coast. The central, most elevated part of the ice sheet has a small SMB increase. The hybrid experiments reveal that most of the SMB reduction is caused directly by the insolation change (cf. iL+oP) with only a minor contribution from the oceanic conditions (mainly in the southwest, cf. iP+oL). The oceanic conditions, however, appear to drive the SMB increase in the southeast.

While no dynamic feedbacks of the ice sheet are included in these estimates, they might still indicate how the simulated changes at 125 ka could impact the ice sheet. The reduced SMB in the north and northeast could be consistent with ice sheet retreat in this region (in line with the reconstructions by Born and Nisancioglu (2012); Quiquet et al. (2013); Stone et al. (2013)). The increased SMB in the southeast further suggests that the ice sheet could persist in southern Greenland and remain connected to the main dome near the current summit, as the accumulation increase seems to overwhelm the impact of the increased temperature.

In summary, our experiments indicate that the insolation change has a stronger impact on the GrIS SMB compared to the SST and sea ice changes. While the oceanic changes cause a larger increase of the annual mean temperature over Greenland (Fig. 5), the impact during summer and thus the contribution to increased melting is limited (cf. Fig. 3). The increased summer melt thus appears to be crucial for the GrIS SMB, as strong SMB reductions are evident in iL+oP, despite the fall and winter cooling. This importance of the Eemian insolation changes for the GrIS SMB, was previous illustrated by van de Berg et al. (2011) based on their regional climate model experiments separating the impacts of changed insolation and changed ambient climate. Despite the fact that the Arctic warming appears stronger in our experiments [comparing EC-Earth (Pedersen et al., 2016b) to the simulated Eemian warming in the ECHO-G model (Cubasch et al., 2006; Kaspar et al., 2007) used as boundary conditions in van de Berg et al. (2011)], the direct impact of the insolation is still the dominant contribution to the GrIS SMB changes. Our results thus similarly illustrate that the relation between warming and GrIS melting during the Eemian is likely not suitable for estimating the ice sheet response to future, greenhouse gas-driven warming. The combined effect of the more seasonally uniform warming and the general snowfall increase driven by the oceanic changes (iP+oL) results in a less pronounced SMB

Clim. Past Discuss., doi:10.5194/cp-2016-48, 2016
Manuscript under review for journal Clim. Past
Published: 26 April 2016

response. In southeastern Greenland, however, the oceanic changes appear to be dominating the SMB response through the increased snowfall and accumulation (Fig. 6).

4 Conclusions

In line with previous model studies (Braconnot et al., 2012; Lunt et al., 2013; Masson-Delmotte et al., 2013; Otto-Bliesner et al., 2013), our simulations underestimate the warming compared to the NEEM ice core reconstructions. While we do take into account the precipitation seasonality impact on the recorded temperature signal, our model simulations have other limitations that might contribute to the model–data discrepancy. These are, in particular, related to the fixed present-day ice sheet topography.

Firstly, a decrease of the ice sheet elevation would increase the near-surface temperature following the atmospheric lapse rate. Secondly, local circulation might be affected by altered ice sheet topography. Merz et al. (2014a) suggest that during winter an increased slope of the ice sheet at a given location increases the wind speed and consequently the sensible heat flux towards the surface. They estimate that GrIS topography changes could contribute up to 3.1 K annual mean warming locally at the NEEM location. Changes in the GrIS topography could also further impact the precipitation patterns and thus increase the summer weight in the precipitation-weighted temperature (Merz et al., 2014b).

Our experiments show that the oceanic changes are contributing considerably to the GrIS warming. The warming even reaches the interior, elevated part of the ice sheet (including the NEEM site). Especially changes in sea ice can affect both the warming, the circulation, and the precipitation, and the GrIS changes are thus sensitive to both the magnitude and the location of sea ice loss (Merz et al., 2016; Pedersen et al., 2016a). Thus, the particular model's sea ice sensitivity and reference state may impact the warming. Despite the substantial Arctic warming, our simulations suggest that the Eemian Arctic sea ice extent was slightly larger than the present (e.g. in the Baffin Bay); further sea ice reduction, especially in the vicinity of Greenland, could further increase GrIS warming (Pedersen et al., 2016a). Based on precipitation-weighted temperature estimates, our hybrid simulations indicate that the combined effect of sea ice loss and SST increase is responsible for 0.8–1.5 K warming recorded at the NEEM deposition site (annual mean temperatures indicate a warming impact of 1.9–2.5 K). In comparison, Merz et al. (2016) estimate that uncertainty in the sea ice cover can account for 1.6 K annual mean warming at the NEEM site.

The hybrid simulations illustrate that the largest contribution to the annual mean Greenland warming is due to oceanic changes. At the NEEM deposition site, the insolation changes favor changes in the precipitation seasonality that increase the summer weight in the precipitation-weighted temperature. Consequently, the isolated impacts of insolation and the associated oceanic changes on the precipitation-weighted temperature are comparable, despite the fact that the oceanic changes cause about 2 K higher annual mean warming. The SMB calculations revealed that while the oceanic changes favor increased accumulation over the southeastern GrIS, the changed insolation causes increased melting and appears to be the dominant factor behind the expected reduction of the GrIS. This reiterates the finding of van de Berg et al. (2011), that direct use of the relation between temperature and mass loss in the Eemian is likely to overestimate future greenhouse gas-driven melting.

Clim. Past Discuss., doi:10.5194/cp-2016-48, 2016
Manuscript under review for journal Clim. Past
Published: 26 April 2016

Acknowledgements. The authors thank Valérie Masson-Delmotte for valuable discussions. Acknowledgement is made for the use of ECMWF's computing and archive facilities in this research. The research leading to these results has received funding from the European Research Council under the European Union's Seventh Framework Programme (FP7/2007–2013)/ERC Grant Agreement 610055 as part of the ice2ice project. The authors acknowledge the support of the Danish National Research Foundation through the Centre for Ice and Climate at the Niels Bohr Institute.

Clim. Past Discuss., doi:10.5194/cp-2016-48, 2016
Manuscript under review for journal Clim. Past
Published: 26 April 2016

Climate of the Past Discussions
Open Access
EGU

References

Berger, A.: Long-term variations of daily insolation and Quaternary climatic changes, Journal of the Atmospheric Sciences, 35, 2362–2367, 1978.

Born, A. and Nisancioglu, K. H.: Melting of Northern Greenland during the last interglaciation, The Cryosphere, 6, 1239–1250, doi:10.5194/tc-6-1239-2012, 2012.

Braconnot, P., Harrison, S. P., Kageyama, M., Bartlein, P. J., Masson-Delmotte, V., Abe-Ouchi, A., Otto-Bliesner, B. L., and Zhao, Y.: Evaluation of climate models using palaeoclimatic data, Nature Climate Change, 2, 417–424, doi:10.1038/nclimate1456, 2012.

CAPE-Last Interglacial Project Members: Last Interglacial Arctic warmth confirms polar amplification of climate change, Quaternary Science Reviews, 25, 1383–1400, doi:10.1016/j.quascirev.2006.01.033, 2006.

Colville, E. J., Carlson, A. E., Beard, B. L., Hatfield, R. G., Stoner, J. S., Reyes, A. V., and Ullman, D. J.: Sr-Nd-Pb Isotope Evidence for Ice-Sheet Presence on Southern Greenland During the Last Interglacial, Science, 333, 620–623, doi:10.1126/science.1204673, 2011.

Cubasch, U., Zorita, E., Kaspar, F., Gonzalez-Rouco, J. F., Storch, H. V., and Prömmel, K.: Simulation of the role of solar and orbital forcing on climate, Advances in Space Research, 37, 1629–1634, doi:10.1016/j.asr.2005.04.076, 2006.

Cuffey, K. M. and Marshall, S. J.: Substantial contribution to sea-level rise during the last interglacial from the Greenland ice sheet, Nature, 404, 591–4, doi:10.1038/35007053, 2000.

Dansgaard, W., Clausen, H. B., Gundestrup, N., Hammer, C. U., Johnsen, S. J., Kristinsdottir, M., and Reeh, N.: A New Greenland Deep Ice Core, Science, 218, 1273–1277, 1982.

Dutton, A. and Lambeck, K.: Ice volume and sea level during the last interglacial., Science, 337, 216–219, doi:10.1126/science.1205749, 2012.

Dutton, A., Carlson, A. E., Long, A. J., Milne, G. A., Clark, P. U., DeConto, R., Horton, B. P., Rahmstorf, S., and Raymo, M. E.: Sea-level rise due to polar ice-sheet mass loss during past warm periods, Science, 349, doi:10.1126/science.aaa4019, 2015.

European Centre for Medium-Range Weather Forecasts: CY36R1 Official IFS Documentation, https://software.ecmwf.int/wiki/display/IFS/CY36R1+Official+IFS+Documentation, 2010.

GRIP members: Climate instability during the last interglacial period recorded in the GRIP ice core, Nature, 364, 203–207, 1993.

Grootes, P. M., Stuiver, M., White, J. W. C., Johnsen, S. J., and Jouzel, J.: Comparison of oxygen isotope records from the GISP2 and GRIP Greenland ice cores, Nature, 366, 552–554, doi:10.1038/366552a0, 1993.

Hakuba, M. Z., Folini, D., Wild, M., and Schr, C.: Impact of Greenland's topographic height on precipitation and snow accumulation in idealized simulations, Journal of Geophysical Research Atmospheres, 117, 1–15, doi:10.1029/2011JD017052, 2012.

Hazeleger, W., Severijns, C., Semmler, T., Ştefănescu, S., Yang, S., Wang, X., Wyser, K., Dutra, E., Baldasano, J. M., Bintanja, R., Bougeault, P., Caballero, R., Ekman, A. M. L., Christensen, J. H., van den Hurk, B., Jimenez, P., Jones, C., Kållberg, P., Koenigk, T., McGrath, R., Miranda, P., Van Noije, T., Palmer, T., Parodi, J. A., Schmith, T., Selten, F., Storelvmo, T., Sterl, A., Tapamo, H., Vancoppenolle, M., Viterbo, P., and Willén, U.: EC-Earth: A Seamless Earth-System Prediction Approach in Action, Bulletin of the American Meteorological Society, 91, 1357–1363, doi:10.1175/2010BAMS2877.1, 2010.

Hazeleger, W., Wang, X., Severijns, C., Ştefănescu, S., Bintanja, R., Sterl, A., Wyser, K., Semmler, T., Yang, S., van den Hurk, B., van Noije, T., van der Linden, E., and van der Wiel, K.: EC-Earth V2.2: description and validation of a new seamless earth system prediction model, Climate Dynamics, 39, 2611–2629, doi:10.1007/s00382-011-1228-5, 2012.

Clim. Past Discuss., doi:10.5194/cp-2016-48, 2016
Manuscript under review for journal Clim. Past
Published: 26 April 2016

Helsen, M. M., van de Berg, W. J., van de Wal, R. S. W., van den Broeke, M. R., and Oerlemans, J.: Coupled regional climate–ice-sheet simulation shows limited Greenland ice loss during the Eemian, Climate of the Past, 9, 1773–1788, doi:10.5194/cp-9-1773-2013, 2013.

Johnsen, S. J., Dahl-Jensen, D., Gundestrup, N., Steffensen, J. P., Clausen, H. B., Miller, H., Masson-Delmotte, V., Sveinbjörnsdottir, A. E., and White, J. W. C.: Oxygen isotope and palaeotemperature records from six Greenland ice-core stations: Camp Century, Dye-3, GRIP, GISP2, Renland and NorthGRIP, Journal of Quaternary Science, 16, 299–307, doi:10.1002/jqs.622, 2001.

Jouzel, J., Alley, R. B., Cuffey, K. M., Dansgaard, W., Grootes, P., Hoffmann, G., Johnsen, S. J., Koster, R. D., Peel, D., Shuman, C. A., Stievenard, M., Stuiver, M., and White, J.: Validity of the temperature reconstruction from water isotopes in ice cores, Journal of Geophysical Research, 102, 26 471–26 487, doi:10.1029/97JC01283, 1997.

Kaspar, F., Spangehl, T., and Cubasch, U.: Northern hemisphere winter storm tracks of the Eemian interglacial and the last glacial inception, Climate of the Past, 3, 181–192, doi:10.5194/cp-3-181-2007, 2007.

Kopp, R. E., Simons, F. J., Mitrovica, J. X., Maloof, A. C., and Oppenheimer, M.: Probabilistic assessment of sea level during the last interglacial stage., Nature, 462, 863–7, doi:10.1038/nature08686, 2009.

Landais, A., Masson-Delmotte, V., Capron, E., Langebroek, P. M., Bakker, P., Stone, E. J., Merz, N., Raible, C. C., Fischer, H., Orsi, A., Prié, F., Vinther, B., and Dahl-Jensen, D.: How warm was Greenland during the last interglacial period?, Climate of the Past Discussions, doi:10.5194/cp-2016-28, 2016.

Langen, P. L., Mottram, R. H., Christensen, J. H., Boberg, F., Rodehacke, C. B., Stendel, M., van As, D., Ahlstrøm, A. P., Mortensen, J., Rysgaard, S., Petersen, D., Svendsen, K. H., Aðalgeirsdóttir, G., and Cappelen, J.: Quantifying Energy and Mass Fluxes Controlling Godthåbsfjord Freshwater Input in a 5-km Simulation (1991–2012), Journal of Climate, 28, 3694–3713, doi:10.1175/JCLI-D-14-00271.1, 2015.

Lefebre, F., Gallée, H., van Ypersele, J.-P., and Greuell, W.: Modeling of snow and ice melt at ETH Camp (West Greenland): A study of surface albedo, Journal of Geophysical Research, 108, doi:10.1029/2001JD001160, 2003.

Lhomme, N., Clarke, G. K., and Marshall, S. J.: Tracer transport in the Greenland Ice Sheet: constraints on ice cores and glacial history, Quaternary Science Reviews, 24, 173–194, doi:10.1016/j.quascirev.2004.08.020, 2005.

Lunt, D. J., de Noblet-Ducoudré, N., and Charbit, S.: Effects of a melted Greenland ice sheet on climate, vegetation, and the cryosphere, Climate Dynamics, 23, 679–694, doi:10.1007/s00382-004-0463-4, 2004.

Lunt, D. J., Abe-Ouchi, A., Bakker, P., Berger, A., Braconnot, P., Charbit, S., Fischer, N., Herold, N., Jungclaus, J. H., Khon, V. C., Krebs-Kanzow, U., Langebroek, P. M., Lohmann, G., Nisancioglu, K. H., Otto-Bliesner, B. L., Park, W., Pfeiffer, M., Phipps, S. J., Prange, M., Rachmayani, R., Renssen, H., Rosenbloom, N., Schneider, B., Stone, E. J., Takahashi, K., Wei, W., Yin, Q., and Zhang, Z. S.: A multi-model assessment of last interglacial temperatures, Climate of the Past, 9, 699–717, doi:10.5194/cp-9-699-2013, 2013.

Masson-Delmotte, V., Braconnot, P., Hoffmann, G., Jouzel, J., Kageyama, M., Landais, A., Lejeune, Q., Risi, C., Sime, L. C., Sjolte, J., Swingedouw, D., and Vinther, B. M.: Sensitivity of interglacial Greenland temperature and δ18O: ice core data, orbital and increased CO2 climate simulations, Climate of the Past, 7, 1041–1059, doi:10.5194/cp-7-1041-2011, 2011.

Masson-Delmotte, V., Schulz, M., Abe-Ouchi, A., Beer, J., Ganopolski, A., González Rouco, J. F., Jansen, E., Lambeck, K., Luterbacher, J., Naish, T., Osborn, T., Otto-Bliesner, B., Quinn, T., Ramesh, R., Rojas, M., Shao, X., and Timmermann, A.: Information from Paleoclimate Archives, in: Climate Change 2013: The Physical Science Basis. Contribution of Working Group I to the Fifth Assessment Report of the Intergovernmental Panel on Climate Change, edited by Stocker, T. F., Qin, D., Plattner, G.-K., Tignor, M., Allen, S. K., Boschung, J., Nauels, A., Xia, Y., Bex, V., and Midgley, P. M., pp. 383–464, Cambridge University Press, doi:10.1017/CBO9781107415324.013, 2013.

Clim. Past Discuss., doi:10.5194/cp-2016-48, 2016
Manuscript under review for journal Clim. Past
Published: 26 April 2016

Merz, N., Born, A., Raible, C. C., Fischer, H., and Stocker, T. F.: Dependence of Eemian Greenland temperature reconstructions on the ice sheet topography, Climate of the Past, 10, 1221–1238, doi:10.5194/cp-10-1221-2014, 2014a.

Merz, N., Gfeller, G., Born, A., Raible, C. C., Stocker, T. F., and Fischer, H.: Influence of ice sheet topography on Greenland precipitation during the Eemian interglacial, Journal of Geophysical Research: Atmospheres, 119, 10 749–10 768, doi:10.1002/2014JD021940.Received, 2014b.

Merz, N., Born, A., Raible, C. C., and Stocker, T. F.: Warm Greenland during the last interglacial: the role of regional changes in sea ice cover, Climate of the Past Discussions, pp. 1–37, doi:10.5194/cp-2016-12, 2016.

Muschitiello, F., Zhang, Q., Sundqvist, H. S., Davies, F. J., and Renssen, H.: Arctic climate response to the termination of the African Humid Period, Quaternary Science Reviews, 125, 91–97, doi:10.1016/j.quascirev.2015.08.012, 2015.

NEEM community members: Eemian interglacial reconstructed from a Greenland folded ice core, Nature, 493, 489–94, doi:10.1038/nature11789, 2013.

NGRIP members: High-resolution record of Northern Hemisphere climate extending into the last interglacial period., Nature, 431, 147–51, doi:10.1038/nature02805, 2004.

Otto-Bliesner, B. L., Rosenbloom, N., Stone, E. J., McKay, N. P., Lunt, D. J., Brady, E. C., and Overpeck, J. T.: How warm was the last interglacial? New model-data comparisons., Philosophical transactions. Series A, Mathematical, physical, and engineering sciences, 371, doi:10.1098/rsta.2013.0097, 2013.

Pedersen, R. A., Cvijanovic, I., Langen, P. L., and Vinther, B. M.: The Impact of Regional Arctic Sea Ice Loss on Atmospheric Circulation and the NAO, Journal of Climate, 29, 889–902, doi:10.1175/JCLI-D-15-0315.1, 2016a.

Pedersen, R. A., Langen, P. L., and Vinther, B. M.: The last interglacial climate – comparing direct and indirect impacts of insolation changes, Submitted to Climate Dynamics, 2016b.

Persson, A., Langen, P. L., Ditlevsen, P. D., and Vinther, B. M.: The influence of precipitation weighting on interannual variability of stable water isotopes in Greenland, Journal of Geophysical Research: Atmospheres, 116, 1–13, doi:10.1029/2010JD015517, 2011.

Petersen, G. N., Kristjánsson, J. E., and Ólafsson, H.: Numerical simulations of Greenland's impact on the Northern Hemisphere winter circulation, Tellus, Series A: Dynamic Meteorology and Oceanography, 56, 102–111, doi:10.1111/j.1600-0870.2004.00047.x, 2004.

Quiquet, A., Ritz, C., Punge, H. J., and Salas y Mélia, D.: Greenland ice sheet contribution to sea level rise during the last interglacial period: a modelling study driven and constrained by ice core data, Climate of the Past, 9, 353–366, doi:10.5194/cp-9-353-2013, 2013.

Robinson, A., Calov, R., and Ganopolski, A.: Greenland ice sheet model parameters constrained using simulations of the Eemian Interglacial, Climate of the Past, 7, 381–396, doi:10.5194/cp-7-381-2011, 2011.

Sime, L. C., Risi, C., Tindall, J. C., Sjolte, J., Wolff, E. W., Masson-Delmotte, V., and Capron, E.: Warm climate isotopic simulations: what do we learn about interglacial signals in Greenland ice cores?, Quaternary Science Reviews, 67, 59–80, doi:10.1016/j.quascirev.2013.01.009, 2013.

Steen-Larsen, H. C., Masson-Delmotte, V., Sjolte, J., Johnsen, S. J., Vinther, B. M., Bréon, F.-M., Clausen, H. B., Dahl-Jensen, D., Falourd, S., Fettweis, X., Gallée, H., Jouzel, J., Kageyama, M., Lerche, H., Minster, B., Picard, G., Punge, H. J., Risi, C., Salas, D., Schwander, J., Steffen, K., Sveinbjörnsdottír, A. E., Svensson, A., and White, J.: Understanding the climatic signal in the water stable isotope records from the NEEM shallow firn/ice cores in northwest Greenland, Journal of Geophysical Research Atmospheres, 116, 1–20, doi:10.1029/2010JD014311, 2011.

Steig, E. J., Grootes, P. M., and Stuiver, M.: Seasonal Precipitation Timing and Ice Core Records, Science, 266, 1885–1886, doi:10.1126/science.266.5192.1885, 1994.

Stone, E. J., Lunt, D. J., Annan, J. D., and Hargreaves, J. C.: Quantification of the Greenland ice sheet contribution to Last Interglacial sea level rise, Climate of the Past, 9, 621–639, doi:10.5194/cp-9-621-2013, 2013.

van de Berg, W. J., van den Broeke, M. R., Ettema, J., van Meijgaard, E., and Kaspar, F.: Significant contribution of insolation to Eemian melting of the Greenland ice sheet, Nature Geoscience, 4, 679–683, doi:10.1038/ngeo1245, 2011.

Vihma, T.: Effects of Arctic Sea Ice Decline on Weather and Climate: A Review, Surveys in Geophysics, 35, 1175–1214, doi:10.1007/s10712-014-9284-0, 2014.

Vinther, B. M., Buchardt, S. L., Clausen, H. B., Dahl-Jensen, D., Johnsen, S. J., Fisher, D. A., Koerner, R. M., Raynaud, D., Lipenkov, V., Andersen, K. K., Blunier, T., Rasmussen, S. O., Steffensen, J. P., and Svensson, A.: Holocene thinning of the Greenland ice sheet, Nature, 461, 385–8, doi:10.1038/nature08355, 2009.

Vionnet, V., Brun, E., Morin, S., Boone, A., Faroux, S., Le Moigne, P., Martin, E., and Willemet, J.-M.: The detailed snowpack scheme Crocus and its implementation in SURFEX v7.2, Geoscientific Model Development, 5, 773–791, doi:10.5194/gmd-5-773-2012, 2012.

von Storch, H. and Zwiers, F. W.: Statistical Analysis in Climate Research, Cambridge University Press, Cambridge, United Kingdom and New York, NY, USA, 2001.

Willerslev, E., Cappellini, E., Boomsma, W., Nielsen, R., Hebsgaard, M. B., Brand, T. B., Hofreiter, M., Bunce, M., Poinar, H. N., Dahl-Jensen, D., Johnsen, S., Steffensen, J. P., Bennike, O., Schwenninger, J.-L., Nathan, R., Armitage, S., de Hoog, C.-J., Alfimov, V., Christl, M., Beer, J., Muscheler, R., Barker, J., Sharp, M., Penkman, K. E. H., Haile, J., Taberlet, P., Gilbert, M. T. P., Casoli, A., Campani, E., and Collins, M. J.: Ancient biomolecules from deep ice cores reveal a forested southern Greenland., Science, 317, 111–114, doi:10.1126/science.1141758, 2007.

Zuo, Z. and Oerlemans, J.: Modelling albedo and specific balance of the Greenland ice sheet: calculations for the Søndre Strømfjord transect, Journal of Glaciology, 42, 305–317, 1996.

Clim. Past Discuss., doi:10.5194/cp-2016-48, 2016
Manuscript under review for journal Clim. Past
Published: 26 April 2016

Climate of the Past Discussions
Open Access
EGU

Tables

Table 1. Boundary conditions for the experiments. In the experiment names, the letter following "i" indicates the insolation conditions, while the letter following "o" indicates the oceanic conditions: "P" is PI and "L" is Eemian (Last Interglacial).

Experiment	Insolation and GHGs	SSTs and sea ice
iP+oP	Pre-industrial	Pre-industrial
iL+oL	Eemian	Eemian
iL+oP	Eemian	Pre-industrial
iP+oL	Pre-industrial	Eemian

Table 2. Annual mean (T_{ann}) and precipitation-weighted (T_{pw}) temperature change relative to iP+oL and associated standard deviations (σ_{ann}, σ_{pw}) for dNEEM. *Not statistically significant at the 95 % confidence level.

Experiment	ΔT_{ann}	σ_{ann}	ΔT_{pw}	σ_{pw}
iL+oL	**2.3 K**	1.5 K	**2.4 K**	3.1 K
iL+oP	**-0.2 K***	1.3 K	**1.6 K**	2.7 K
iP+oL	**1.9 K**	1.4 K	**1.5 K**	2.6 K

Clim. Past Discuss., doi:10.5194/cp-2016-48, 2016
Manuscript under review for journal Clim. Past
Published: 26 April 2016

Climate of the Past
Discussions
Open Access
EGU

Figures

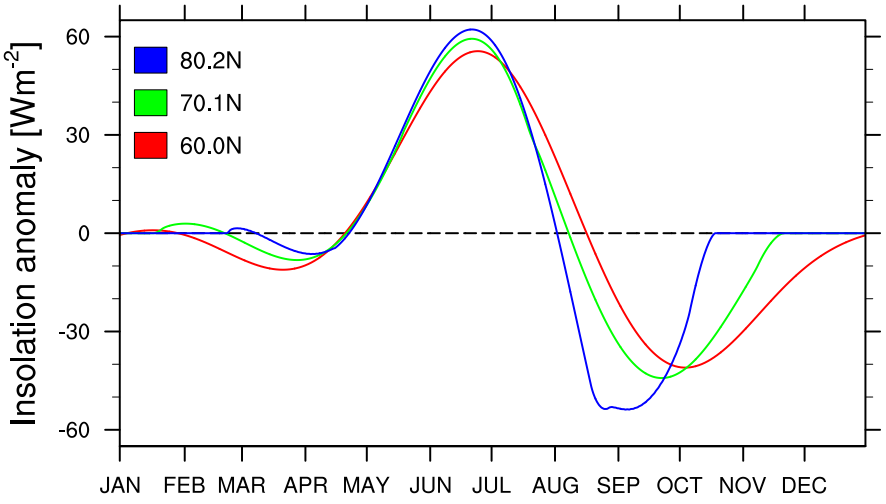

Figure 1. Insolation anomalies [Wm^{-2}] in Eemian relative to PI. The selected latitudes represent southern (60° N, red), middle (70° N, green), and northern (80° N, blue) Greenland. Tick marks indicate the beginning of each month.

Clim. Past Discuss., doi:10.5194/cp-2016-48, 2016
Manuscript under review for journal Clim. Past
Published: 26 April 2016

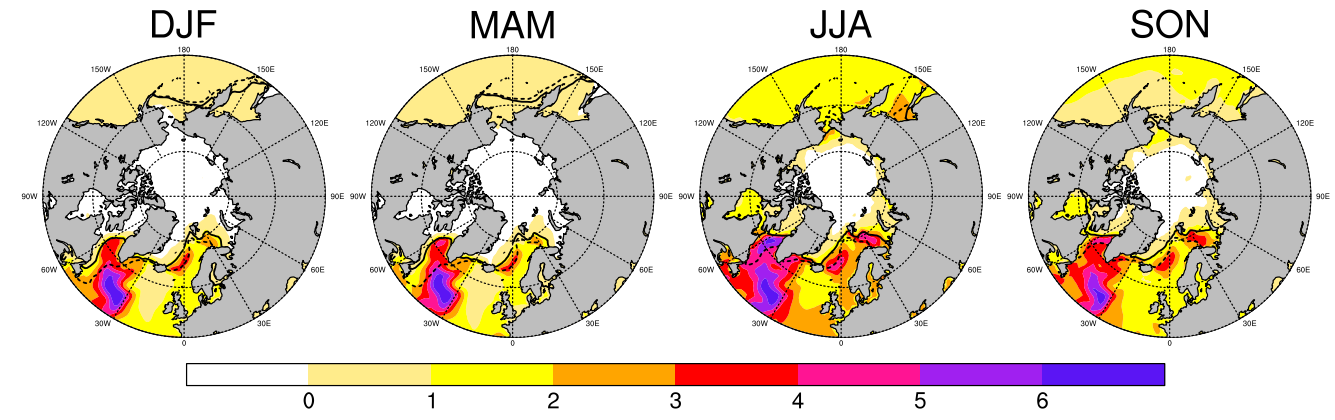

Figure 2. Seasonal mean SST anomalies [K] in Eemian relative to PI boundary conditions. Black contours indicate the sea ice extent (i.e. the 15 % concentration contour): PI (dashed) and Eemian (solid).

Clim. Past Discuss., doi:10.5194/cp-2016-48, 2016
Manuscript under review for journal Clim. Past
Published: 26 April 2016

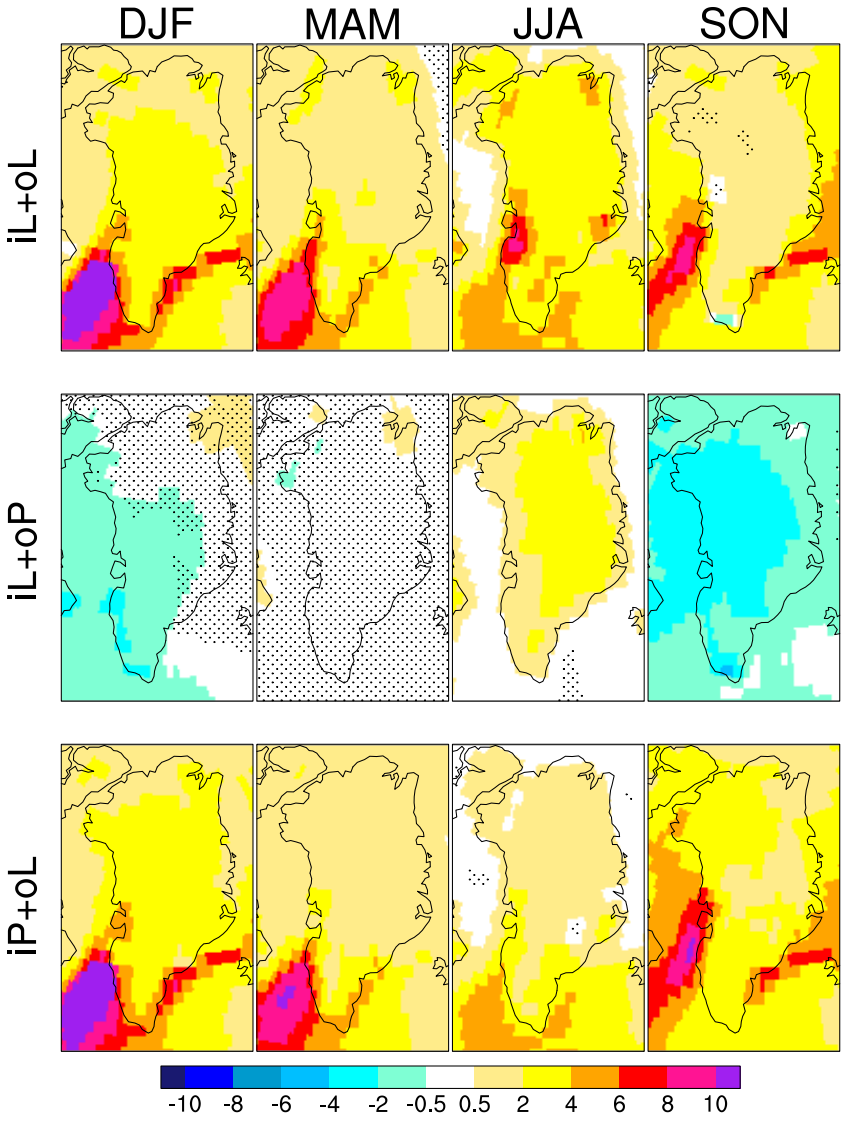

Figure 3. Seasonal mean near-surface temperature anomalies [K] compared to iP+oP in the three experiments: iL+oL (top), iL+oP (middle), and iP+oL (bottom). Only changes larger than ±0.5 K are shown. Black dotted shading marks anomalies that are not statistically significant at the 95 % level.

Clim. Past Discuss., doi:10.5194/cp-2016-48, 2016
Manuscript under review for journal Clim. Past
Published: 26 April 2016

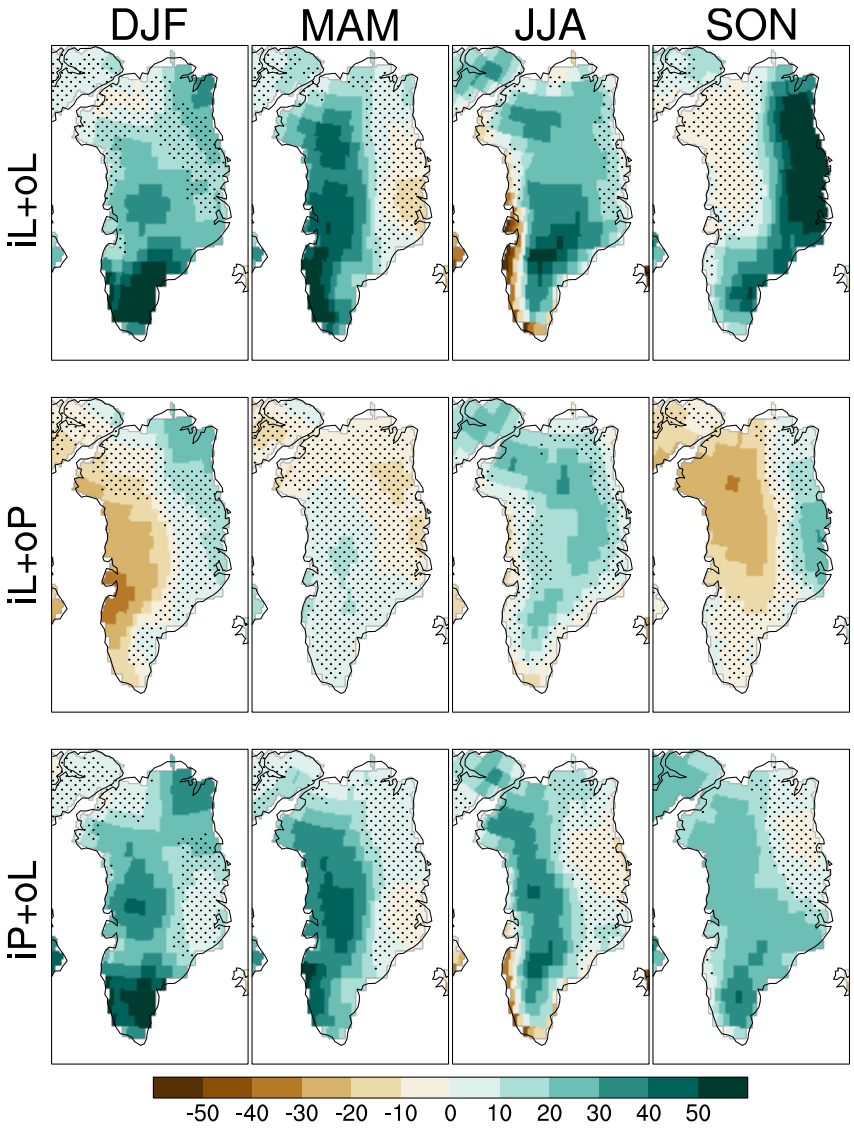

Figure 4. Seasonal mean relative snowfall anomalies [%] from iP+oP: iL+oL (top), iL+oP (middle), and iP+oL (bottom). Black dotted shading marks anomalies that are not statistically significant at the 95 % level.

Clim. Past Discuss., doi:10.5194/cp-2016-48, 2016
Manuscript under review for journal Clim. Past
Published: 26 April 2016

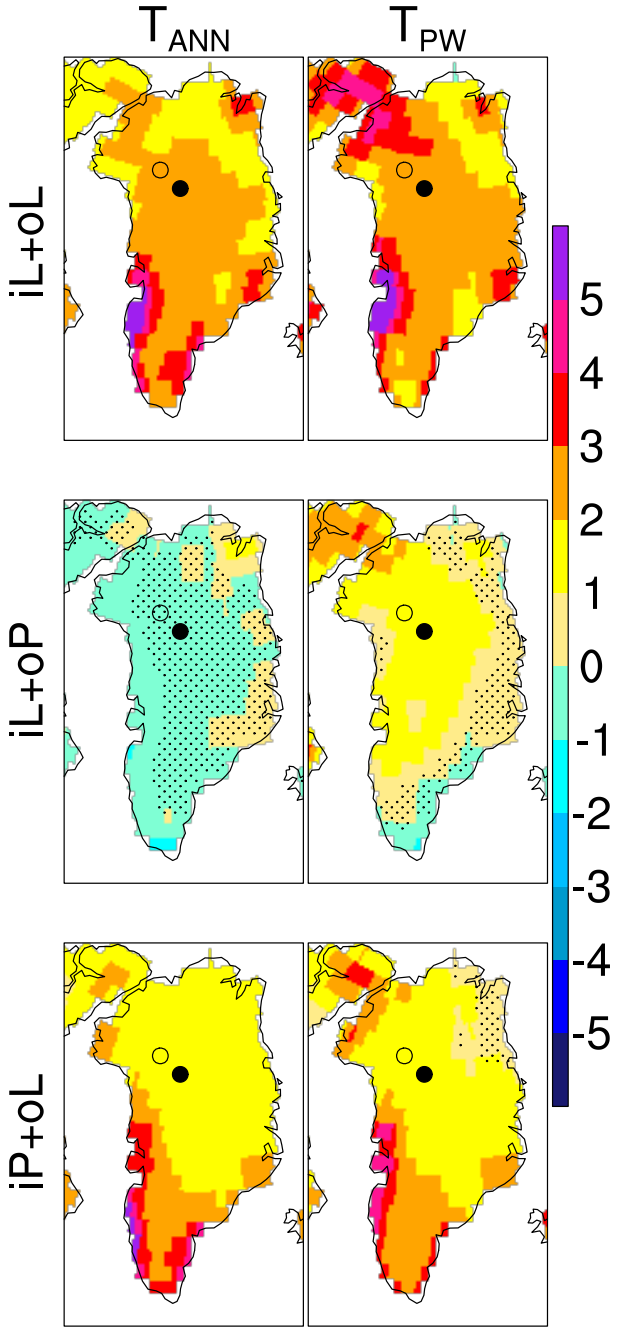

Figure 5. Near-surface air temperature anomalies [K] in iL+oL (top), iL+oP (mid), and iP+oL (bottom) compared to iP+oP: Annual mean (left column) and precipitation-weighted mean (right column). Black dotted shading marks anomalies that are not statistically significant at the 95 % level. dNEEM (NEEM) location is marked with the filled (hollow) black circle. Note the changed color bar compared to the seasonal means.

Clim. Past Discuss., doi:10.5194/cp-2016-48, 2016
Manuscript under review for journal Clim. Past
Published: 26 April 2016

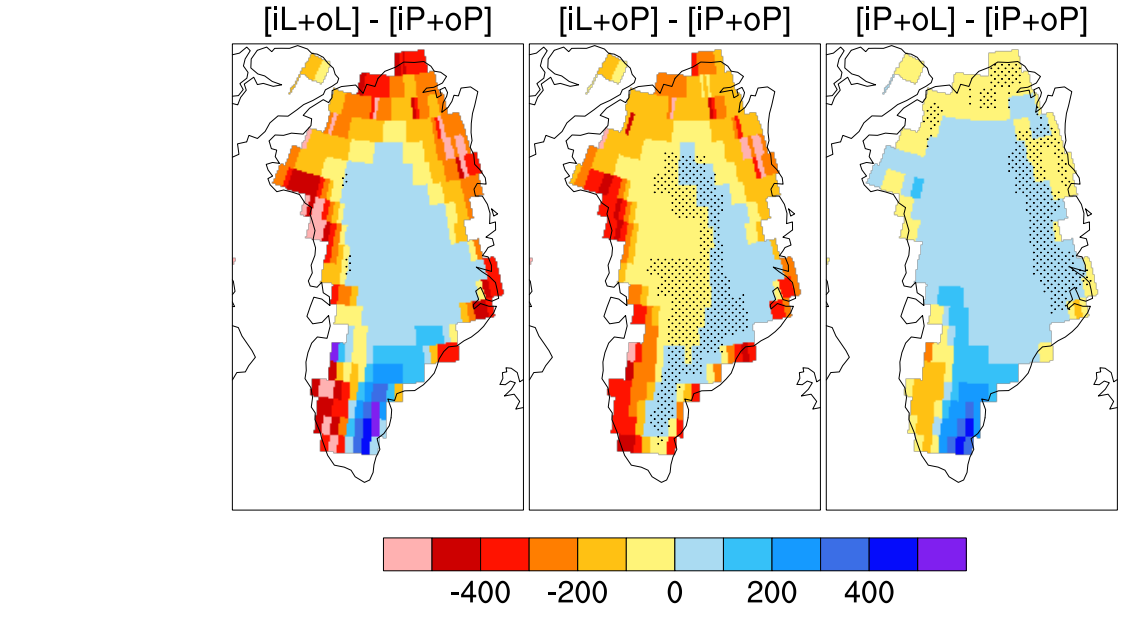

Figure 6. Surface mass balance anomalies [mm water-equivalent] compared to iP+oP: iL+oL (left), iL+oP (center), and iP+oL (right). Black dotted shading marks anomalies that are not significant at the 95 % confidence level.